Somatic Activating *PIK3CA* Mutations Cause Venous Malformation

Nisha Limaye,[1] Jaakko Kangas,[2,6] Antonella Mendola,[1,6] Catherine Godfraind,[3,4] Matthieu J. Schlögel,[1] Raphael Helaers,[1] Lauri Eklund,[2] Laurence M. Boon,[1,5] and Miikka Vikkula[1,*]

Somatic mutations in *TEK*, the gene encoding endothelial cell tyrosine kinase receptor TIE2, cause more than half of sporadically occurring unifocal venous malformations (VMs). Here, we report that somatic mutations in *PIK3CA*, the gene encoding the catalytic p110α subunit of PI3K, cause 54% (27 out of 50) of VMs with no detected *TEK* mutation. The hotspot mutations c.1624G>A, c.1633G>A, and c.3140A>G (p.Glu542Lys, p.Glu545Lys, and p.His1047Arg), frequent in *PIK3CA*-associated cancers, overgrowth syndromes, and lymphatic malformation (LM), account for >92% of individuals who carry mutations. Like VM-causative mutations in *TEK*, the *PIK3CA* mutations cause chronic activation of AKT, dysregulation of certain important angiogenic factors, and abnormal endothelial cell morphology when expressed in human umbilical vein endothelial cells (HUVECs). The p110α-specific inhibitor BYL719 restores all abnormal phenotypes tested, in *PIK3CA*- as well as *TEK*-mutant HUVECs, demonstrating that they operate via the same pathogenic pathways. Nevertheless, significant genotype-phenotype correlations in lesion localization and histology are observed between individuals with mutations in *PIK3CA* versus *TEK*, pointing to gene-specific effects.

Venous malformations (VMs) are localized developmental defects composed of ectatic venous channels with a thin endothelial cell (EC) lining, surrounded by sparse, erratically distributed vascular smooth muscle cells (vSMCs) and a disorganized extracellular matrix (ECM).[1,2] VMs cause aesthetic problems, chronic and significant pain, and obstruction of organ function as a result of their size or localization. Currently, they are treated with surgery, sclerotherapy, or both; however, these approaches have significant limitations, including inaccessibility of lesions and regrowth after incomplete resection.[1]

We discovered that activating mutations in *TEK*, the gene encoding the EC tyrosine kinase receptor TIE2 (MIM 600221), cause familial[3,4] (MIM 600195) as well as sporadically occurring VMs,[5,6] and downstream PI3K/AKT signaling represents a major effector mechanism in lesion formation.[2,7,8] This led to the first evidence-based application of molecular therapy to VMs: inhibition of the PI3K/AKT pathway by the mTOR inhibitor rapamycin (sirolimus) proved effective in ameliorating disease in a mouse model as well as a pilot cohort of individuals with difficult-to-treat VMs.[8]

PI3K signaling is initiated by binding of the p85 regulatory subunit to phosphorylated tyrosine residues of ligand-activated receptors, allowing for the activation of the p110 catalytic subunit.[9] Chronic PI3K/AKT activation can instead occur as a result of somatic mutations in *PIK3CA* (the gene encoding p110α, a class IA PI3K catalytic protein; MIM 171834). Such mutations have been identified in a wide variety of cancers[10,11] (Catalogue of Somatic Mutations in Cancer; COSMIC); in overgrowth syndromes,[12–16] some of which (congenital lipomatous overgrowth with vascular, epidermal, and skeletal anomalies [CLOVES][17] (MIM 612918); Klippel-Trenaunay syndrome [KTS][18] (MIM 149000); Fibro-adipose vascular anomaly [FAVA][18]) have a vascular component;[19] and in lymphatic malformation (LM[18,20,21]). Given the pivotal role of PI3K activation in VM causation, we hypothesized that *PIK3CA* mutations might cause VMs that lack detectable TIE2 alterations.[5,6]

We screened surgically excised VMs from 87 unrelated individuals with unifocal VM. Informed consent was obtained from all participants, as approved by the ethics committee of the Faculty of Medicine at Université Catholique de Louvain. Tissues were collected in liquid nitrogen immediately after surgical excision, performed for reasons of medical necessity only. Frozen tissue homogenization was followed by overnight digestion with 100 μg/ml Proteinase K at 56° and DNA extraction (Wizard Genomic DNA extraction kit, Promega). Targeted deep sequencing of the 23 *TEK* and 20 *PIK3CA* coding exons (with ten nucleotides of flanking introns each) was carried out with an Ion AmpliSeq Custom DNA Panel (Life Technologies), which consists of primers for multiplexed PCR amplification of regions of interest (100% coverage of *TEK*; 98.75% coverage, missing 11 nucleotides in and flanking exon 5 and 34 nucleotides in exon 20, of *PIK3CA*). Ion Ampliseq libraries (with unique molecular bar codes and universal priming sequences ligated to each PCR-amplified sample according to manufacturers' instructions) were pooled, loaded onto an Ion 316 Chip V2, and sequenced on an Ion PGM (all from Life Technologies) according to manufacturers' instructions. Raw sequences (FASTQ files) were separated by bar code and aligned to the human genome reference sequence (assembly GRCh37/hg19) by the Torrent Server (Life Technologies). Aligned sequence (BAM) files were submitted to the Torrent Variant Caller

[1]Human Molecular Genetics, de Duve Institute, Université Catholique de Louvain, 1200 Brussels, Belgium; [2]Oulu Center for Cell-Matrix Research, Faculty of Biochemistry and Molecular Medicine, Biocenter Oulu, University of Oulu, 90014 Oulu, Finland; [3]Clermont Université, Université d'Auvergne, 63000 Clermont-Ferrand, France; [4]Service d'Anatomopathologie, Hôpital Gabriel Montpied, Centre Hospitalier Universitaire Clermont-Ferrand, 63000 Clermont-Ferrand, France; [5]Center for Vascular Anomalies, Division of Plastic Surgery, Cliniques Universitaires Saint-Luc and Université Catholique de Louvain, 1200 Brussels, Belgium; [6]These authors contributed equally to this work
*Correspondence: miikka.vikkula@uclouvain.be
http://dx.doi.org/10.1016/j.ajhg.2015.11.011.

Table 1. Somatic Mutations Identified in Individuals with Unifocal VM

Study	*TEK* Mutation Detected			*PIK3CA* Mutation Detected	*TEK*, *PIK3CA* Mutation Not Detected	Total Screened
	c.2740C>T (p.Leu914Phe)	Other	Total			
Limaye et al., 2009[5]	24	2	26	-	-	-
Soblet et al., 2013[6]	9	8	17	-	-	-
Current study	26	11	37	27	23[a]	-
Total (percent of total screened)	59 (73.8%[b])	21 (26.2%[b])	80 (61.5%)	27 (20.8%)	23 (17.7%)	130

[a]All samples without a detected *TEK* mutation from previous studies (by Sanger-sequencing of tissue cDNA[5,6]) were included in the current study.
[b]Percent of samples with a *TEK* mutation.

for variant calling (Life Technologies). Called variants were subsequently annotated, filtered, and visualized with Highlander, an in-house bioinformatics framework.

The following quality-control criteria were used in calling a sample positive for a variant: (1) total coverage depth of $\geq$100 reads across the position; (2) $\geq$5 mutant reads, including both forward and reverse orientation reads; and (3) $\geq$1% mutant read frequency. Variants that passed these criteria were evaluated as follows: (1) synonymous variants were discarded; (2) variants present at >1% frequency in databases of known polymorphisms (1000 Genomes, Genome of the Netherlands [GoNL], NHLBI Exome Sequencing Project (ESP 2500 and 6500), and Exome Aggregation Consortium [ExAC]) were discarded. Novel missense mutations were submitted to six programs (Polyphen2; SIFT; Mutation Taster; Mutation Assessor; Functional Analysis though Hidden Markov Models, or FATHMM; and Likelihood Ratio Test, or LRT; all implemented in Highlander) for their predicted effect on protein function.

We identified *PIK3CA* mutations in affected tissues from 27 out of 87 screened individuals (31%), and we identified *TEK* mutations in 37 individuals (Table 1). When combined with previously published data,[5,6] mutations in *TEK* account for 80 out of 130 (61.5%) individuals with unifocal VM (Table 1); c.2740C>T (NM_000459.4; p.Leu914Phe) remains the most frequent mutation (74%; Table 1). *PIK3CA* mutations account overall for 27 out of 130 individuals with unifocal VM (20.8%; Table 1).

Five *PIK3CA* mutations were detected, at allele frequencies ranging from 1% to 17.5% of total reads (Figure 1, Table S1). "Hotspot" mutations (the most recurrent mutations in *PIK3CA*-associated cancers and developmental disorders) were identified in 25 out of the 27 individuals with *PIK3CA* mutations (Figure 1): The p110 α-helical-domain substitutions p.Glu542Lys (c.1624G>A, NM_006218.2) and p.Glu545Lys (c.1633G>A) were identified in eight and four individuals, respectively (together, 44.4%). The kinase domain substitution p.His1047Arg (c.3140A>G) was identified in 13 individuals (48.1%). p.Gly118Asp (c.353G>A) and p.Gln546His (c.1638G>T), both present in the COSMIC database, were identified in one individual each (Figure 1, Table S1). p.Gly118Asp is predicted to be damaging to protein function by six out of six in silico prediction programs, and p.Gln546His is predicted to be damaging by 3 out of 6 programs.

Targeted deep sequencing was performed on all available blood DNA from individuals with *PIK3CA* mutations identified in lesions. Blood DNA from an individual was considered positive for the variant detected in the corresponding tissue if (1) the variant was present in $\geq$5 reads, (2) the total read depth was $\geq$100 reads, and (3) the variant was detected at $\geq$3 SDs above the mean background frequency, calculated separately for each variant position, as described in Table S1.

PIK3CA mutations were not detected in affected individuals' blood DNA, despite coverage depths ranging from 383–11,384 reads (mean: 4,940) across the five mutation positions (Table S1). Added to the relatively low frequency of mutant alleles detected in tissues (Table S1), this suggests that VM-causative *PIK3CA* mutations are indeed somatic.

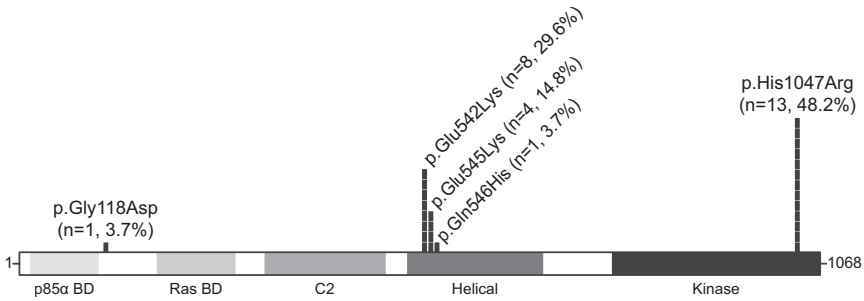

Figure 1. Distribution of Amino Acid Changes and Frequency of *PIK3CA* Somatic Mutations in Unifocal VM-Affected Individuals
PIK3CA protein domains with mutations identified and their frequency (percentage) among individuals with somatic *PIK3CA* mutations. Abbreviations are as follows: n, number of individuals; BD, binding domain.

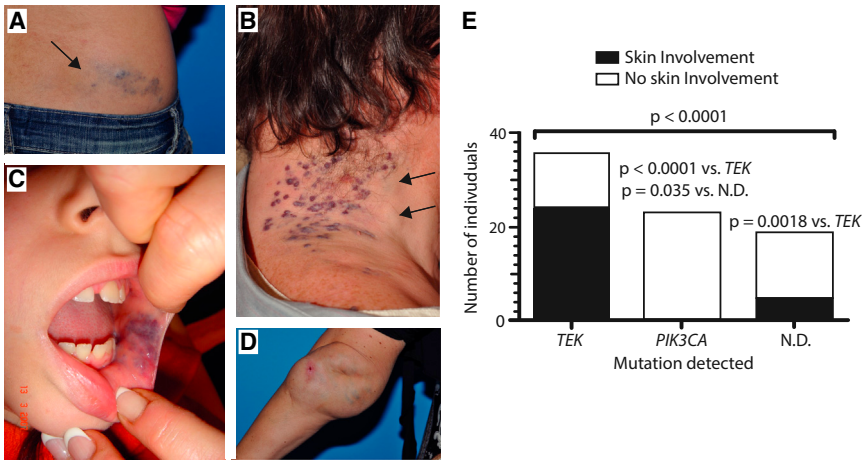

Figure 2. VM Localization in Individuals with Mutations Detected in *TEK*, *PIK3CA*, or Neither

Single, extensive slow-flow malformations, present at birth and growing proportionately with individual. Lesions are bluish and compressible. They can be cutaneous (A and B), sub-cutaneous (A and B, arrows; D), mucosal (C), or extended deep into muscles (intra-muscular), joints (intra-articular, (D) or other tissues and organs. (A and B) Skin involvement; (C, D) no skin involvement. (E) Number of VMs with a mutation detected in *TEK*, *PIK3CA*, or neither (N.D.: none detected) that do or do not show skin involvement ($p < 0.0001$ overall, chi-square test). Inter-group p values: post-hoc Fisher's exact tests.

VMs are often cutaneous (Figures 2A and 2B), subcutaneous (Figures 2A and 2B), or mucosal (Figure 2C) and can extend deep into various tissues and organs, such as muscles, joints (Figure 2D), and intestines. We observed that in subjects with *TEK* mutations (n = 37 identified in this study; Table 1), VMs often affected, but were not restricted to, the skin (24 out of 36 individuals for whom information on lesion localization was available; 66.7%). By contrast, of the 23 (out of 27) *PIK3CA*-associated VMs with available localization information, none showed skin involvement (Figure 2C). This suggests that, unlike *TEK*-associated VMs, *PIK3CA*-associated VMs tend not to extend to the skin surface, perhaps as result of differences in where and when these mutations were acquired.

VMs, uniquely among vascular anomalies, are associated with significant coagulopathy in the form of high D-dimer levels, sometimes accompanied by low fibrinogen levels.[1,22,23] We found that D-dimer levels were significantly lower in individuals with no detected *TEK* or *PIK3CA* mutations than in individuals with mutations in either gene (Figure S1). D-dimer levels have been correlated with total lesion size;[22] this might therefore simply reflect differences in the surface area, depth, or volume of VMs caused by *TEK* and *PIK3CA* mutations, as compared to those of as-yet-unknown cause. Alternatively, it could be due to dysregulation of coagulation cascade components in the endothelium; we demonstrate that such effects can be engendered by *TEK*[2] and *PIK3CA* mutations (current study) in human umbilical vein endothelial cells (HUVECs).

Blinded histological evaluation of hematoxylin and eosin-stained formalin-fixed and paraffin-embedded tissue sections from 36 unifocal VMs revealed four distinct categories (Figure 3A): the majority (n = 24), placed in category I, consisted of isolated or interconnected veins with large, highly irregular lumens and thick fibrotic walls containing irregularly distributed clumps of vSMCs running parallel to the ECs; their characteristics corresponding to the "classic" histological description of the malformation. Eight VMs, placed in category II, were similar to VMs observed in *PTEN* hamartoma tumor syndrome (PHTS; MIM 601728) and were characterized by interconnected veins with fibrotic walls containing foci of lymphoid cells and vSMCs radiating outward in irregular bundles perpendicular to the lumen. The minority of VMs were placed in categories III (n = 2) and IV (n = 2), both characterized by small, dilated veins with thick walls composed of regular layers of vSMCs. Veins in category III were isolated, whereas those in category IV were smaller and clustered together; individual lumens were separated by fibrous tissue, and a thick vSMC layer bordered the entire cluster. 18 out of 21 tissues with *TEK* mutations (75%) were in category I, whereas only two were in category II and only 1 was in category III. In contrast, tissues with *PIK3CA* mutations were equally distributed between categories I and II (three and four out of seven, respectively), and none were in categories III or IV. Intriguingly, categories III and IV were almost exclusively made up of samples with no detected *TEK* and *PIK3CA* mutation. Samples without a detected mutation also included three tissues in category I and two in category II (Figure 3E).

We previously showed that *TEK* mutations cause cell-intrinsic alterations when expressed in HUVECs[2,5,8] and that activation of PI3K/AKT is a universal feature of HUVECs expressing mutated *TEK*.[2,7] We hypothesized that, because *PIK3CA* encodes the major isoform mediating growth-factor-induced PI3K activation in ECs,[24] *PIK3CA* mutations have similar effects. HUVECs were retrovirally transfected with *PIK3CA* wild-type or recurrent VM-causative mutant forms (c.1624G>A, c.1633G>A, and c.3140A>G [p.Glu542Lys, p.Glu545Lys, and p.His1047Arg]) in the pMXs-puro vector.[27] Similar to the most common VM-causative mutant, *TEK* c.2740C>T (TIE2 p.Leu914Phe[2,7,8]), PIK3CA variants activated AKT (Figure 4A), disrupted normal EC-characteristic monolayer morphology as visualized by phase-contrast microscopy (Figure 4B), resulted in loss of ECM fibronectin (Figure 4C), and strongly downregulated *ANGPT2* and *PDGF-B* mRNA expression as measured by real-time quantitative PCR with normalization to *GAPDH* (Figure 4D). Plasminogen system-components were also somewhat dysregulated by PIK3CA variants (Figure 4D). Inhibition of

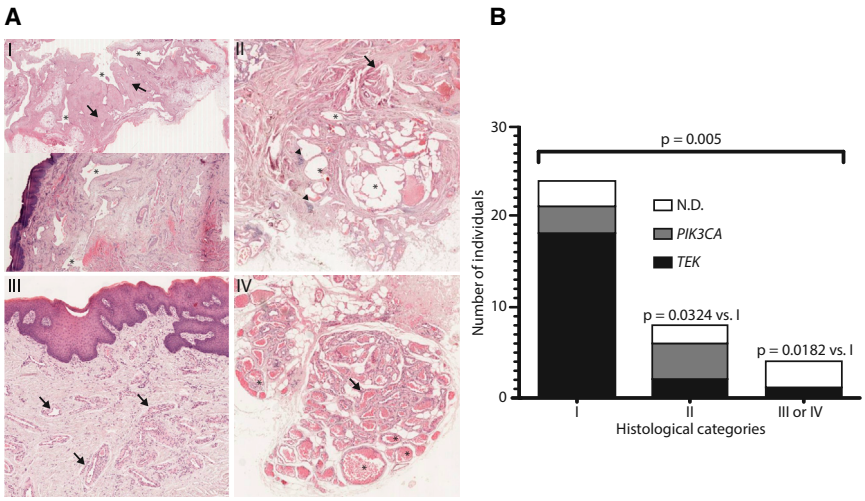

Figure 3. Histological Categorization of Unifocal VM Tissues

(A) Hematoxylin and eosin-stained sections demonstrating the major features of four histological categories identified. (I) Interconnected (top) or isolated (bottom) veins with large, irregular lumens (asterisks) and thick fibrotic walls (arrows) containing irregular vascular smooth-muscle-cell aggregates (not visible at this magnification) oriented in parallel with ECs; (II) interconnected veins (asterisks) with fibrotic walls containing radial bundles of vascular smooth-muscle cells (arrow) and foci of lymphoid cells (arrowheads); (III, IV) small-to-medium sized dilated veins (asterisks) with thick walls composed of organized layers of vascular smooth-muscle cells (arrows), either isolated (III) or clustered with fibrous tissue separating lumens (IV).

(B) Number of samples with a mutation detected in *TEK*, *PIK3CA*, or neither (N.D.: none detected) in each histological category ($p = 0.005$ overall, chi-square test). Inter-group p values: post-hoc chi-square tests.

PIK3CA with BYL7129, which selectively targets p110α,[25] abolished both PIK3CA-variant and TIE2-p.Leu914Phe-induced AKT phosphorylation (Figure 5A), indicating that these proteins participate in the same signaling pathway. In addition, PIK3CA inhibition restored cell morphology (Figures 5C and 5D) and ECM fibronectin levels (Figure 5E) in both PIK3CA- and TIE2-p.Leu914Phe variants. Collectively, these data indicate that TIE2 and PIK3CA variants induce the same VM-causative signaling pathways.

Interestingly, unlike TIE2-p.Leu914Phe,[2,7] PIK3CA variants induced low levels of pSTAT1 when they were compared to the wild-type, and they induced no pERK1/2 (Figure 4A). Added to the phenotypic differences observed between individuals with *TEK* versus *PIK3CA* mutations, this suggests certain gene-specific features that are yet to be understood.

Rapamycin, probably because of its inhibitory effect on AKT phosphorylation, was shown to control VM growth in a murine transplantation model, and it had therapeutic benefits in a clinical pilot study of six individuals (five with VM and one with KTS).[8] Three individuals with VM had a *TEK* mutation,[8] and the remaining three (one individual with KTS and individuals 10 and 57 with VMs; Table S1) were found to have a *PIK3CA* mutation. We compared the effects of BYL719 and rapamycin on abnormal HUVEC phenotypes. Rapamycin diminished AKT phosphorylation but did not restore ECM fibronectin to wild-type levels in PIK3CA-variant or TIE2-p.Leu914Phe HUVECs (Figures 5B and 5E). Loss of the EC cobblestone pattern was not, however, rescued in either PIK3CA-variant or TIE2-p.Leu914Phe HUVECs (Figure 5C). This could be because PI3K activation, in addition to leading to changes in the AKT/mTOR pathway, leads to wider changes in kinase activity in pathways including MAPK and ErbB;[26] only a subset of these changes are probably reversed by rapamycin.

We previously showed that TIE2-mediated VMs from mouse transplant models and affected individuals have features (revealed by histology and electron microscopy) that correspond well to HUVEC-intrinsic phenotypes observed in vitro.[2,8] These include an uneven endothelial layer with prominent cellular elongations and abnormal perivascular ECM characterized by a wide basement membrane with randomly oriented, isolated collagen fibrils and irregularly distributed vSMCs.[2] Downregulation of PDGF-B, which we demonstrated ex vivo in VM tissue sections from affected individuals,[7] most likely contributes to defective recruitment of vSMCs. Downregulation of ANGPT2 might contribute to decreased sprouting (with increased lumen expansion)[2] by abnormal ECs, whereas ECM alterations are associated with upregulation of serine proteases, including tissue plasminogen activator (tPA/PLAT) and urokinase-type plasminogen activator (uPA).[2] Induction of the plasmin/plasminogen cascade (tPA and uPA upregulation with Plasminogen Activator Inhibitor 1 (PAI1) downregulation[2]) might also contribute to increased fibrinolysis and elevated levels of D-dimers in individuals with VM.[1,22,23] PIK3CA inhibition reverses all abnormal features of PIK3CA- and TIE2-variant HUVECs. It therefore represents an attractive potential therapy for TIE2- and PIK3CA-mediated disease, which together account for the majority (82%) of unifocal VMs.

Accession Numbers

The accession number for the 108 sequences (*TEK* and *PIK3CA* coding exons from 87 tissue samples and 21 blood samples) reported in this paper is PRJEB11395, available at European Nucleotide Archive.

Supplemental Data

Supplemental Data include one figure and one table and can be found with this article online at http://dx.doi.org/10.1016/j.ajhg.2015.11.011.

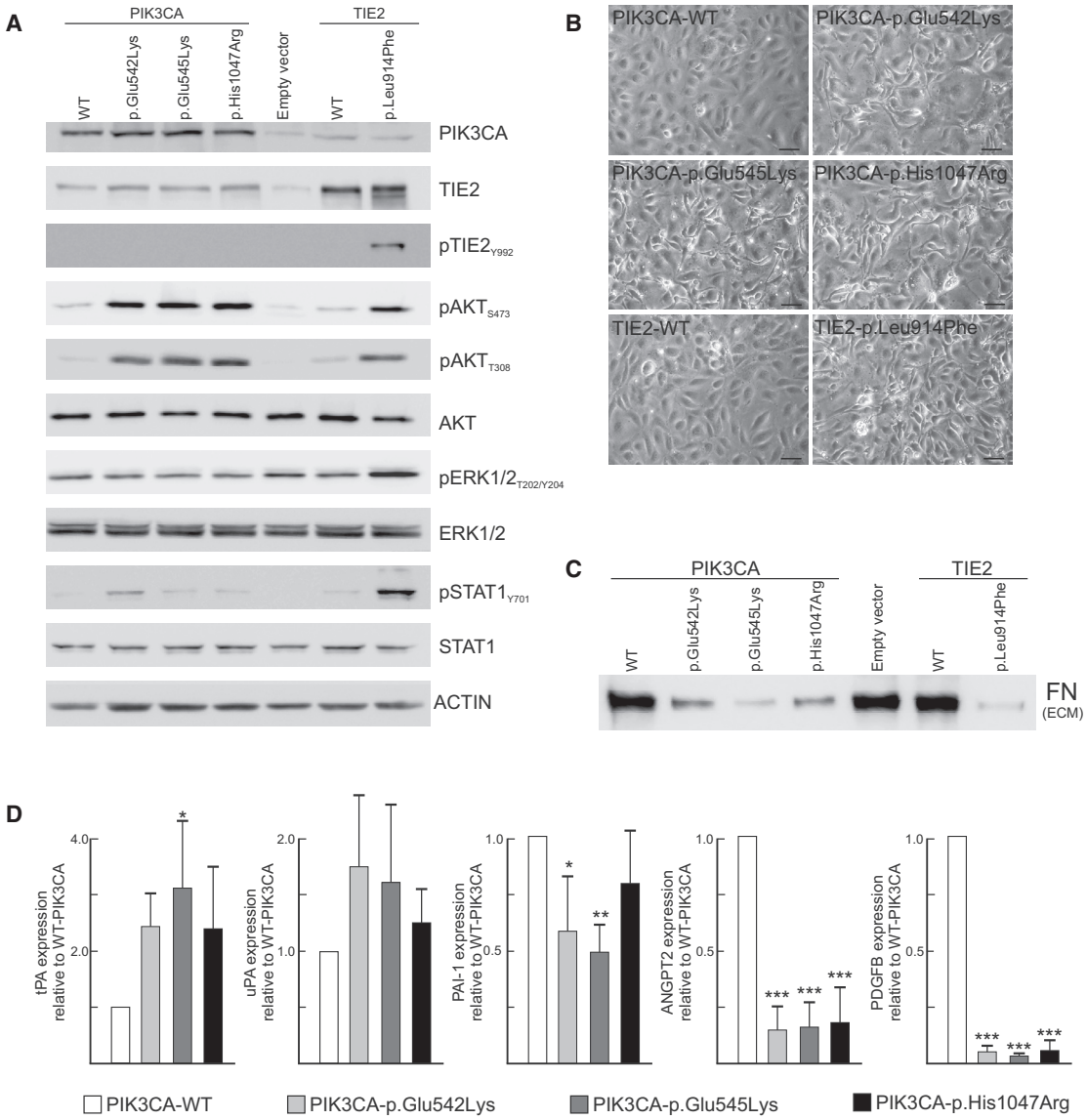

Figure 4. VM-Causative PIK3CA and TIE2 Variants Cause Similar Phenotypes in Transduced HUVECs
Full-length cDNAs encoding TIE2-WT and TIE2-Leu914Phe cloned into pMXs vector, full-length cDNAs for PIK3CA-WT cloned into pMXs-puro retroviral vector,[27] and mutations generated with the QuikChange Site-Directed Mutagenesis Kit (Agilent Technologies) according to the manufacturer's protocol. 293-GPG-VSV-G viral packaging cells[28] were transfected with Fugene HD transfection reagent (Promega) to produce viruses. HUVECs were transduced with pMXs-puro-PIK3CA constructs or empty vector selected with 1 μg/ml puromycin (Sigma) for 5 days. (**A**) Activation of signaling molecules by HUVECs retrovirally transduced to express variant and wild-type proteins. A representative immunoblot from three independent experiments is shown.
(B) Elongated cell morphology with loss of cobblestone pattern in PIK3CA- and TIE2-variant HUVECs (the scale bar represents 50 μm).
(**C**) Loss of ECM fibronectin: representative immunoblot from three independent experiments. HUVECs were removed by washing with 0.05% Triton X-100 and 50 mM NH4OH in PBS, followed by one wash with 50 mM NH4OH and three washes with PBS. Lysis was carried out with ECM lysis buffer (6.5M Urea, 9.1 mM Na_2HPO_4, 1.7 mM NaH_2PO_4, 1% NP-40, 0.25% Sodium Deoxycholate, 150 mM NaCl, 0.1% SDS, and 1 mM EDTA).
(D) Normalized n-fold change in gene expression measured by real-time quantitative PCR on HUVEC cDNA (means + SD, *$p < 0.05$, **$p < 0.01$, ***$p < 0.001$ versus PIK3CA-WT, ANOVA with Tukey's post-hoc test). WT indicates wild-type.

Acknowledgments

We are grateful to all the participants and their family members. These studies were partially supported by funding from the Belgian Science Policy Office Interuniversity Attraction Poles (BELSPO-IAP) program through the project IAP P7/43-BeMGI; the National Institutes of Health, Program Project P01 AR048564 (both to M.V.); the Fonds de la Recherche Scientifique (FRS-FNRS) under Grant T.0026.14 (to M.V.); and the Academy of Finland (136880 and Centre of Excellence Program 2012–2017 to L.E.). We also thank la Communauté Française de Wallonie-Bruxelles and la Lotterie Nationale, Belgium for their support. N.L. is a "Chercheur Qualifié du FRS-FNRS." We thank the genetics platform of Université Catholique de Louvain for access to the IonTorrent Next Generation Sequencer. The authors thank Ms. Liliana Niculescu for secretarial help.

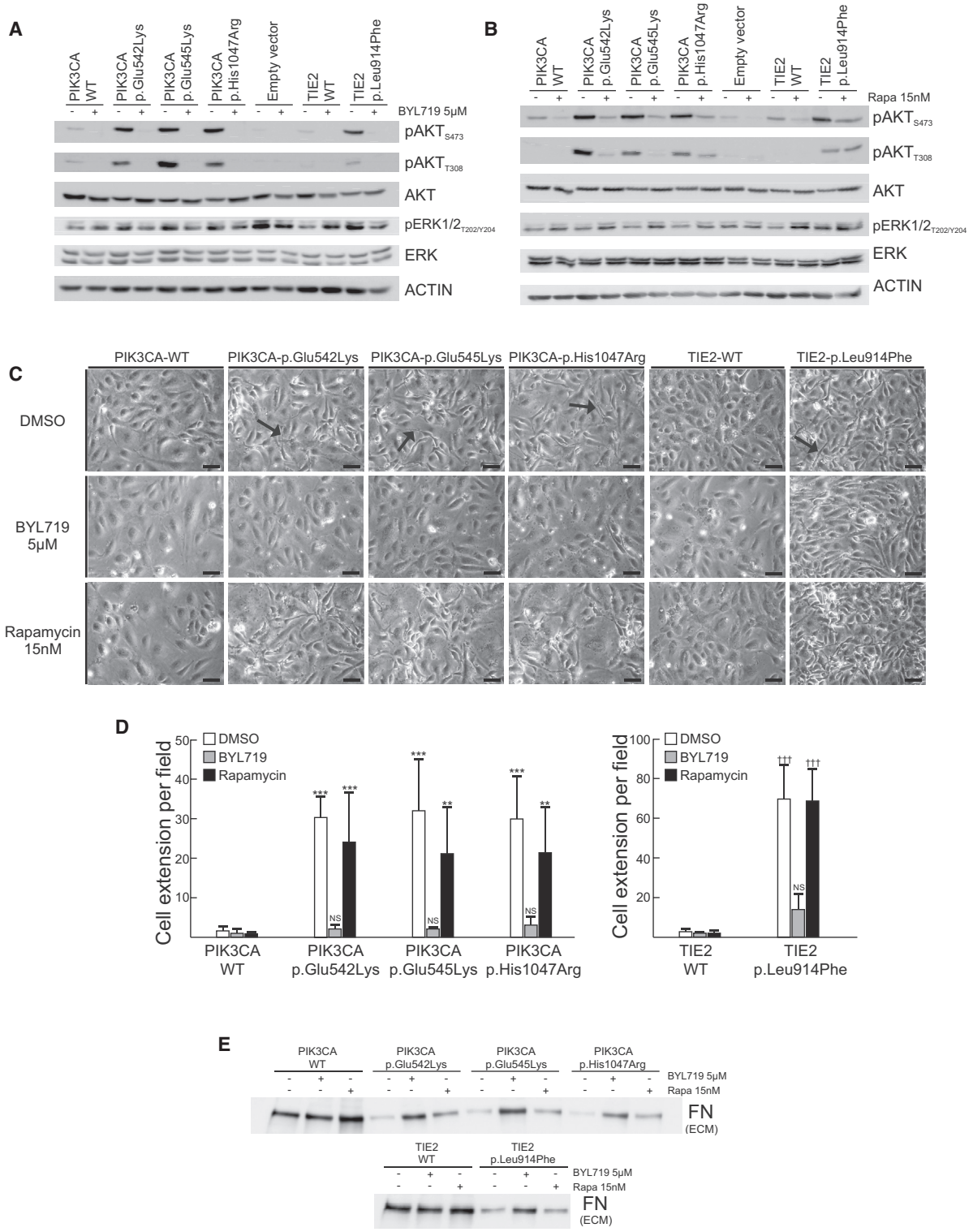

Figure 5. Normalization of PIK3CA- and TIE2-Variant HUVEC Phenotypes by PIK3CA Inhibition

(A) Effect of PIK3CA (p110α) inhibitor BYL719 versus DMSO control on AKT and ERK1/2 phosphorylation in confluent PIK3CA- and TIE2-variant cells at 24 hr in full-serum media; a representative immunoblot from two independent experiments is shown.

(B) Effect of mTOR inhibitor rapamycin versus DMSO control on AKT and ERK1/2 phosphorylation in confluent PIK3CA- and TIE2-variant cells at 24 hr in full-serum media; a representative immunoblot from two independent experiments is shown.

(C and D) Effects of DMSO (control), BYL719, or rapamycin on cell morphology at 24 hr. Cell extensions (arrows) were quantitated from digital images; representative images from four independent experiments are shown. The scale bar represents 50 μm. Three images per dish were randomly captured with a phase-contrast microscope, and the number of thin cell extensions overlapping neighboring cells was manually counted from digitalized images. The average number of extensions from three images was considered a single

(legend continued on next page)

Received: October 10, 2015
Accepted: November 4, 2015
Published: December 3, 2015

Web Resources

The URLs for data presented herein are as follows:

1000 Genomes, http://www.1000genomes.org/
COSMIC, http://cancer.sanger.ac.uk/cosmic
European Nucleotide Archive accession number, http://www.ebi.ac.uk/ena/data/view/PRJEB11395
Exome Aggregation Consortium (ExAC), http://exac.broadinstitute.org/
Functional Analysis though Hidden Markov Models (FATHMM), http://fathmm.biocompute.org.uk/
Genome of the Netherlands (GoNL), http://www.nlgenome.nl/
Highlander, http://sites.uclouvain.be/highlander/
Mutation Assessor, http://mutationassessor.org/
Mutation Taster, http://www.mutationtaster.org/
NHLBI Exome Sequencing Project (ESP), http://evs.gs.washington.edu/EVS/
Online Mendelian Inheritance in Man (OMIM), http://www.omim.org
Polyphen2, http://genetics.bwh.harvard.edu/pph2/
SIFT, http://sift.jcvi.org/

References

1. Dompmartin, A., Vikkula, M., and Boon, L.M. (2010). Venous malformation: update on aetiopathogenesis, diagnosis and management. Phlebology *25*, 224–235.
2. Nätynki, M., Kangas, J., Miinalainen, I., Sormunen, R., Pietilä, R., Soblet, J., Boon, L.M., Vikkula, M., Limaye, N., and Eklund, L. (2015). Common and specific effects of TIE2 mutations causing venous malformations. Hum. Mol. Genet. *24*, 6374–6389.
3. Vikkula, M., Boon, L.M., Carraway, K.L., 3rd, Calvert, J.T., Diamonti, A.J., Goumnerov, B., Pasyk, K.A., Marchuk, D.A., Warman, M.L., Cantley, L.C., et al. (1996). Vascular dysmorphogenesis caused by an activating mutation in the receptor tyrosine kinase TIE2. Cell *87*, 1181–1190.
4. Wouters, V., Limaye, N., Uebelhoer, M., Irrthum, A., Boon, L.M., Mulliken, J.B., Enjolras, O., Baselga, E., Berg, J., Dompmartin, A., et al. (2010). Hereditary cutaneomucosal venous malformations are caused by TIE2 mutations with widely variable hyper-phosphorylating effects. Eur. J. Hum. Genet. *18*, 414–420.
5. Limaye, N., Wouters, V., Uebelhoer, M., Tuominen, M., Wirkkala, R., Mulliken, J.B., Eklund, L., Boon, L.M., and Vikkula, M. (2009). Somatic mutations in angiopoietin receptor gene TEK cause solitary and multiple sporadic venous malformations. Nat. Genet. *41*, 118–124.
6. Soblet, J., Limaye, N., Uebelhoer, M., Boon, L.M., and Vikkula, M. (2013). Variable somatic TIE2 mutations in half of sporadic venous malformations. Mol. Syndromol. *4*, 179–183.
7. Uebelhoer, M., Nätynki, M., Kangas, J., Mendola, A., Nguyen, H.L., Soblet, J., Godfraind, C., Boon, L.M., Eklund, L., Limaye, N., and Vikkula, M. (2013). Venous malformation-causative TIE2 mutations mediate an AKT-dependent decrease in PDGFB. Hum. Mol. Genet. *22*, 3438–3448.
8. Boscolo, E., Limaye, N., Huang, L., Kang, K.T., Soblet, J., Uebelhoer, M., Mendola, A., Natynki, M., Seront, E., Dupont, S., et al. (2015). Rapamycin improves TIE2-mutated venous malformation in murine model and human subjects. J. Clin. Invest. *125*, 3491–3504.
9. Thorpe, L.M., Yuzugullu, H., and Zhao, J.J. (2015). PI3K in cancer: divergent roles of isoforms, modes of activation and therapeutic targeting. Nat. Rev. Cancer *15*, 7–24.
10. Samuels, Y., Wang, Z., Bardelli, A., Silliman, N., Ptak, J., Szabo, S., Yan, H., Gazdar, A., Powell, S.M., Riggins, G.J., et al. (2004). High frequency of mutations of the PIK3CA gene in human cancers. Science *304*, 554.
11. Samuels, Y., and Waldman, T. (2010). Oncogenic mutations of PIK3CA in human cancers. Curr. Top. Microbiol. Immunol. *347*, 21–41.
12. Lee, J.H., Huynh, M., Silhavy, J.L., Kim, S., Dixon-Salazar, T., Heiberg, A., Scott, E., Bafna, V., Hill, K.J., Collazo, A., et al. (2012). De novo somatic mutations in components of the PI3K-AKT3-mTOR pathway cause hemimegalencephaly. Nat. Genet. *44*, 941–945.
13. Lindhurst, M.J., Parker, V.E., Payne, F., Sapp, J.C., Rudge, S., Harris, J., Witkowski, A.M., Zhang, Q., Groeneveld, M.P., Scott, C.E., et al. (2012). Mosaic overgrowth with fibroadipose hyperplasia is caused by somatic activating mutations in PIK3CA. Nat. Genet. *44*, 928–933.
14. Rivière, J.B., Mirzaa, G.M., O'Roak, B.J., Beddaoui, M., Alcantara, D., Conway, R.L., St-Onge, J., Schwartzentruber, J.A., Gripp, K.W., Nikkel, S.M., et al.; Finding of Rare Disease Genes (FORGE) Canada Consortium (2012). De novo germline and postzygotic mutations in AKT3, PIK3R2 and PIK3CA cause a spectrum of related megalencephaly syndromes. Nat. Genet. *44*, 934–940.
15. Rios, J.J., Paria, N., Burns, D.K., Israel, B.A., Cornelia, R., Wise, C.A., and Ezaki, M. (2013). Somatic gain-of-function mutations in PIK3CA in patients with macrodactyly. Hum. Mol. Genet. *22*, 444–451.
16. Maclellan, R.A., Luks, V.L., Vivero, M.P., Mulliken, J.B., Zurakowski, D., Padwa, B.L., Warman, M.L., Greene, A.K., and Kurek, K.C. (2014). PIK3CA activating mutations in facial infiltrating lipomatosis. Plast. Reconstr. Surg. *133*, 12e–19e.
17. Kurek, K.C., Luks, V.L., Ayturk, U.M., Alomari, A.I., Fishman, S.J., Spencer, S.A., Mulliken, J.B., Bowen, M.E., Yamamoto, G.L., Kozakewich, H.P., and Warman, M.L. (2012). Somatic mosaic activating mutations in PIK3CA cause CLOVES syndrome. Am. J. Hum. Genet. *90*, 1108–1115.
18. Luks, V.L., Kamitaki, N., Vivero, M.P., Uller, W., Rab, R., Bovée, J.V., Rialon, K.L., Guevara, C.J., Alomari, A.I., Greene, A.K., et al. (2015). Lymphatic and other vascular malformative/overgrowth disorders are caused by somatic mutations in PIK3CA. J. Pediatr. *166*, 1048–54.e1, 5.
19. Keppler-Noreuil, K.M., Sapp, J.C., Lindhurst, M.J., Parker, V.E., Blumhorst, C., Darling, T., Tosi, L.L., Huson, S.M.,

observation. (Mean+ SD, ***$p < 0.001$, **$p < 0.01$ versus PIK3CA-WT DMSO, †††$p < 0.001$, †$p < 0.05$ versus TIE2-WT DMSO, ANOVA followed by Tukey's test).
(E) Effect of BYL719 and rapamycin on ECM fibronectin; a representative immunoblot from two independent experiments is shown. WT indicates wild-type.

Whitehouse, R.W., Jakkula, E., et al. (2014). Clinical delineation and natural history of the PIK3CA-related overgrowth spectrum. Am. J. Med. Genet. A. *164A*, 1713–1733.
20. Boscolo, E., Coma, S., Luks, V.L., Greene, A.K., Klagsbrun, M., Warman, M.L., and Bischoff, J. (2015). AKT hyper-phosphorylation associated with PI3K mutations in lymphatic endothelial cells from a patient with lymphatic malformation. Angiogenesis *18*, 151–162.
21. Osborn, A.J., Dickie, P., Neilson, D.E., Glaser, K., Lynch, K.A., Gupta, A., and Dickie, B.H. (2015). Activating PIK3CA alleles and lymphangiogenic phenotype of lymphatic endothelial cells isolated from lymphatic malformations. Hum. Mol. Genet. *24*, 926–938.
22. Dompmartin, A., Acher, A., Thibon, P., Tourbach, S., Hermans, C., Deneys, V., Pocock, B., Lequerrec, A., Labbé, D., Barrellier, M.T., et al. (2008). Association of localized intravascular coagulopathy with venous malformations. Arch. Dermatol. *144*, 873–877.
23. Dompmartin, A., Ballieux, F., Thibon, P., Lequerrec, A., Hermans, C., Clapuyt, P., Barrellier, M.T., Hammer, F., Labbé, D., Vikkula, M., and Boon, L.M. (2009). Elevated D-dimer level in the differential diagnosis of venous malformations. Arch. Dermatol. *145*, 1239–1244.
24. Graupera, M., Guillermet-Guibert, J., Foukas, L.C., Phng, L.K., Cain, R.J., Salpekar, A., Pearce, W., Meek, S., Millan, J., Cutillas, P.R., et al. (2008). Angiogenesis selectively requires the p110alpha isoform of PI3K to control endothelial cell migration. Nature *453*, 662–666.
25. Furet, P., Guagnano, V., Fairhurst, R.A., Imbach-Weese, P., Bruce, I., Knapp, M., Fritsch, C., Blasco, F., Blanz, J., Aichholz, R., et al. (2013). Discovery of NVP-BYL719 a potent and selective phosphatidylinositol-3 kinase alpha inhibitor selected for clinical evaluation. Bioorg. Med. Chem. Lett. *23*, 3741–3748.
26. Wu, X., Renuse, S., Sahasrabuddhe, N.A., Zahari, M.S., Chaerkady, R., Kim, M.S., Nirujogi, R.S., Mohseni, M., Kumar, P., Raju, R., et al. (2014). Activation of diverse signalling pathways by oncogenic PIK3CA mutations. Nat. Commun. *5*, 4961.
27. Kitamura, T., Koshino, Y., Shibata, F., Oki, T., Nakajima, H., Nosaka, T., and Kumagai, H. (2003). Retrovirus-mediated gene transfer and expression cloning: powerful tools in functional genomics. Exp. Hematol. *31*, 1007–1014.
28. Ory, D.S., Neugeboren, B.A., and Mulligan, R.C. (1996). A stable human-derived packaging cell line for production of high titer retrovirus/vesicular stomatitis virus G pseudotypes. Proc. Natl. Acad. Sci. USA *93*, 11400–11406.